International Journal of Mechanical, Industrial and Aerospace Sciences
ISSN: 2517-9950
Vol:2, No:5, 2008

# Simulation of Roughness Shape and Distribution Effects on Rarefied and Compressible Flows at Slip Flow Regime

M. Hakak Khadem, S. Hossainpour, and M. Shams

***Abstract*—**A numerical simulation of micro *Poiseuille* flow has performed for rarefied and compressible flow at slip flow regimes. The wall roughness is simulated in two cases with triangular microelements and random micro peaks distributed on wall surfaces to study the effects of roughness shape and distribution on flow field. Two values of Mach and Knudsen numbers have used to investigate the effects of rarefaction as well as compressibility. The numerical results have also checked with available theoretical and experimental relations and good agreements has achieved. High influence of roughness shape can be seen for both compressible and incompressible rarefied flows. In addition it is found that rarefaction has more significant effect on flow field in microchannels with higher relative roughness. It is also found that compressibility has more significant effects on *Poiseuille number* when relative roughness increases.

***Keywords*—**Relative roughness, slip flow, *Poiseuille number*, roughness distribution.

## I. Introduction

AT microscale level, it is impossible to obtain a completely smooth wall surface. According to the traditional knowledge for macrosystems, when the relative roughness is less than 5%, its effect on the friction factor is negligible. But for microscale channels, previously reported experimental and computational results have drawn a conclusion that surface roughness has a significant influence on flow and heat transfer [1, 2].

However, it has been reported that phenomena in microgeometry may differ from those in macroscopic counterparts. Several factors that are dominant in micro scale have been identified through a number of experimental, analytical and numerical works. Among them, noncontinuum effect, compressibility effect, and various surface effects have been under vigorous investigation.

For example, the experiment by Kandlikar et al. [2] indicated that for a 0.62 mm tube with relative roughness of 0.355%, the effect of roughness on the friction factor and heat transfer was significant. Mala and Li [3] observed that for rough channels with diameters ranging from 50 to 254 lm (relative roughness height 0.7–3.5%), the pressure gradient was higher than that predicted by the classical theory and the friction factor increased when the Re number was increased. In addition, an early transition from laminar to turbulent flow occurred at the Reynolds number less than 2300. They concluded that these phenomena can be well explained due to the surface roughness effects.

In some experimental works such as Wu and Little [4, 5], friction factors have been measured for both laminar and turbulent flows in miniaturized channels etched in silicon and glass. The hydraulic diameter of trapezoidal-cross-section microchannels ranged from 45.46 to 83.08 mm. The measured values of the friction factor were much larger (e.g., 10–30% in silicon channels and 3–5 times in glass channels) than those predicted by the conventional correlation for a smooth circular tube. They attributed their anomalous results to the large relative (and asymmetric) roughness of test channels (actually, the equivalent relative roughness was estimated to be in the range of 0.2 to 0.3 through indirect measurement). Choi et al. [6] measured friction factors of nitrogen flow in microtubes of diameter ranging from 3 to 81 mm. The measured friction factors for laminar and turbulent flows were found to be consistently smaller than those predicted by the macro scale correlation in macro tubes. For laminar flow ($Re < 2300$), the friction constant, C, was 19–27% smaller than the conventional one, with an average friction constant of 53, instead of 64.

In modeling of roughness effect on rarefied flows, Usami et al. [7] studied rarefied gas flow through a 2D channel using a DSMC method by varying the surface roughness distribution and the Kn number. The reduction of flow conductivity caused by surface roughness was obtained in the transition regime. Sun's study [8] by using a DSMC method found that the roughness element size had a significant effect on the friction factor of rarefied flows when $0.01 < Kn < 0.1$. Karniadakis et al. [9] applied a more accurate gas flow model

M. Hakak Khadem is with the Mechanical Engineering Department, Sahand University of Technology, Tabriz, Iran (e-mail: masoudhak2007@yahoo.com).

S. Hossainpour is with the Mechanical Engineering Department, Sahand University of Technology, Tabriz, Iran (corresponding author to provide phone: +98-412-3459053; fax: +98-412-3444300; e-mail: hossainpour@sut.ac.ir).

M. Shams is with the Mechanical Engineering Department, K. N. Toosi University of Technology, Tehran, Iran (e-mail: shams@kntu.ac.ir).

and found that the roughness effect becomes more significant on rarefied flows when the Kn number was increased.

However, for a rarefied gas flowing in a microchannel, the roughness effect is more complex and difficult to measure [10]. Experimental investigation by Sugiyama [11,12] demonstrated that the conductance of an unsteady rarified flow between two flat, rough plates decreased significantly with decrease in Kn when Kn > 1. It reached the minimum value around Kn = 0.5, and with further decrease in Kn, the conductance increased rapidly. Their calculation also showed that a pronounced effect of the wave angle on the flow conductance, when Kn = 1 and Kn = 0.1. They did not investigate the roughness effect on rarefied flow in the slip regime (0.001 < Kn < 0.1).

There are also some studies on direct simulation of roughness. Valdes et al [13] have numerically investigated the roughness effect on laminar incompressible flow through microchannels. In their work the roughness is simulated by the superimposition of randomly generated triangular peaks on the inner wall of a smooth microchannel. In recent research Ji et al.[14] studied the influence of roughness in slip flow regime with second order slip boundary conditions. They simulated the roughness with rectangular elements on two parallel plates with different spacing and heights to investigate the effect of wall roughness on friction factor and Nusselt number. They showed that the effect of wall roughness is reduces with increasing Knudsen number.

In this study we will focus on slip flow regime (0.001 < Kn < 0.1) that requires the use of slip boundary conditions. Although there are several models for slip boundary conditions, we will use Maxwell model for slip and Smoluchowskyi for temperature jump conditions that will be discussed later. Compressibility and rarefaction effect on fluid flow will be taken into consideration.

## II. Model Introductions and Problem Statements

### A. Model Development

A pressure-driven gas flow between two long parallel plates has been taken as flow field. Fig. 1a shows a schematic of the *2D* flow through a rough channel with length *L* and height *H*. to simulate roughness on channel surfaces we considered triangular peaks with height *r* and width *w* for two models of case 1. These elements are uniformly and symmetrically distributed on the top and bottom surfaces. Although, this geometry is not exactly the same as the actual rough surface, it is considered as a close approximation to investigate the roughness effect on the flow field and pressure distribution. This was also studied in a work by Ji et al but they assumed roughness as rectangular microelements. We can also simulate roughness with randomly distributed peaks with various heights. Although this seems to be the best approximation for surface roughness, through our knowledge there has been no study on accommodation coefficients in such geometries. Hence there is also case 2, contains two models that roughness elements are randomly distributed on their surfaces (Fig. 2b). The distance between the two plates is considered as *H*, which is also the characteristic length of the flow system. A parameter called *''relative roughness height''* is defined as $e = r/H$. in our simulation r is referred to the average of all roughness elements heights in the domain. In most microfluidic systems, the relative roughness heights are estimated at 0.1–6%. We adopt this roughness height range for the study. From the above discussion, we know that the rarefaction effect cannot be neglected. In addition, for the pressure driven gas flow, when the channel length is much larger than the channel height *(L >> H)*, even in the low Reynolds number range, the Mach number can reach a higher value due to small hydraulic diameter and higher pressure drop.

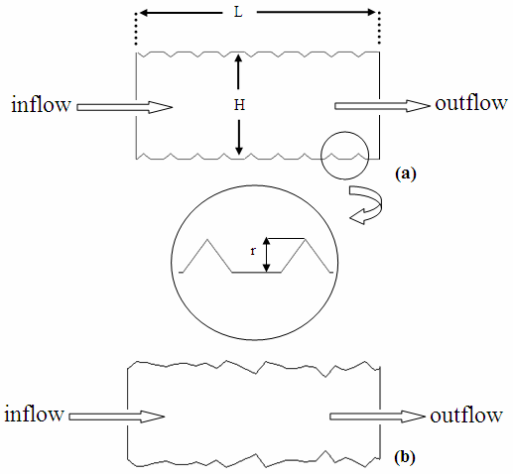


Fig. 1 Microchannels with (a): triangular and (b): random roughness elements. (Both have 5% relative roughness)

### B. Governing Equations

In slip flow regime, for steady laminar flow of compressible fluid with constant thermophysical properties, the governing equations are continuity, momentum, energy and the gas state equations that must be solved with appropriate boundary conditions which will be stated in the next section. These equations have been shown bellow.

$$\frac{\partial(\rho u)}{\partial x}+\frac{(\rho v)}{\partial y}=0 \tag{1}$$

$$\rho u\frac{\partial u}{\partial x}+\rho v\frac{\partial u}{\partial y}=-\frac{\partial P}{\partial x}+\mu\left[\frac{\partial^2 u}{\partial x^2}+\frac{\partial^2 u}{\partial y^2}+\frac{1}{3}\left(\frac{\partial^2 u}{\partial x^2}+\frac{\partial^2 v}{\partial x\partial y}\right)\right] \tag{2}$$

$$\rho u\frac{\partial v}{\partial x}+\rho v\frac{\partial v}{\partial y}=-\frac{\partial P}{\partial y}+\mu\left[\frac{\partial^2 v}{\partial x^2}+\frac{\partial^2 v}{\partial y^2}+\frac{1}{3}\left(\frac{\partial^2 v}{\partial x^2}+\frac{\partial^2 u}{\partial x\partial y}\right)\right] \tag{3}$$

$$\begin{aligned}&\rho c_p u\frac{\partial T}{\partial x}+\rho c_p v\frac{\partial T}{\partial y}=\\&\frac{\partial}{\partial x}\left(K\frac{\partial T}{\partial x}\right)+\frac{\partial}{\partial y}\left(K\frac{\partial T}{\partial y}\right)+u\frac{\partial P}{\partial x}+v\frac{\partial P}{\partial y}\\&+\mu\left[2\left(\frac{\partial u}{\partial x}\right)^2+2\left(\frac{\partial v}{\partial y}\right)^2+\left(\frac{\partial u}{\partial y}+\frac{\partial v}{\partial x}\right)^2\right]-\frac{2}{3}\mu\left(\frac{\partial u}{\partial x}+\frac{\partial v}{\partial y}\right)^2\end{aligned} \tag{4}$$

$$P=\rho RT \tag{5}$$

Where $T, \rho_i$, $P$, $u$ and $v$ are the gas temperature, density, pressure, streamwise velocity, and normal velocity, respectively. $C_p, \mu$ and $K$ are the specific heat, viscosity and thermal conductivity of the gas, which are taken as constant. The above equations are non dimensionalized with respect to the channel height $H$, inlet mean velocity $u_i$, inlet temperature $T_i$, inlet mean density $\rho_i$ and inlet pressure $P_i$. Also some of important dimensionless numbers that have been used are shown bellow:

$$\eta\frac{\partial(\rho^*U)}{\partial X}+\frac{\partial(\rho^*V)}{\partial Y}=0 \tag{6}$$

$$\mathrm{Re}_i\,\rho^*(\eta U\frac{\partial U}{\partial X}+V\frac{\partial V}{\partial Y})= -\frac{\eta\,\mathrm{Re}_i}{\gamma Ma_i^{\,2}}\frac{\partial P^*}{\partial X}+[\eta^2\frac{\partial^2U}{\partial X^2}+\frac{\partial^2U}{\partial Y^2}+\frac{1}{3}(\eta^2\frac{\partial^2U}{\partial X^2}+\eta\frac{\partial^2V}{\partial X\partial Y})] \tag{7}$$

$$\mathrm{Re}_i\,\rho^*(\eta U\frac{\partial V}{\partial X}+V\frac{\partial V}{\partial Y})= -\frac{\eta\,\mathrm{Re}_i}{\gamma Ma_i^{\,2}}\frac{\partial P^*}{\partial Y}+[\eta^2\frac{\partial^2V}{\partial X^2}+\frac{\partial^2V}{\partial Y^2}+\frac{1}{3}(\eta^2\frac{\partial^2V}{\partial X^2}+\eta\frac{\partial^2U}{\partial X\partial Y})] \tag{8}$$

$$\eta U\frac{\partial\theta}{\partial X}+V\frac{\partial\theta}{\partial Y}= \frac{1}{Pe_i\rho^*}[\eta^2\frac{\partial}{\partial X}(\frac{\partial\theta}{\partial X})+\frac{\partial}{\partial Y}(\frac{\partial\theta}{\partial Y})+Ec_i\frac{P_i}{\rho_i u_i^{\,2}\rho^*}[\eta U\frac{\partial P}{\partial X}+V\frac{\partial P}{\partial Y}] +\frac{Ec_i}{\mathrm{Re}_i\rho^*}[2(\frac{\partial U}{\partial X}\eta)^2+2(\frac{\partial V}{\partial Y})^2+(\frac{\partial V}{\partial X}\eta+\frac{\partial U}{\partial Y})^2-\frac{2}{3}(\frac{\partial U}{\partial X}\eta+\frac{\partial V}{\partial Y})^2] \tag{9}$$

Where the parameters for non-dimensionalizing are:

$$\theta=\frac{T-T_w}{T_i-T_w},\ \eta=\frac{H}{L},\ X=\frac{x}{L},\ Y=\frac{y}{H},\ \rho^*=\frac{\rho}{\rho_i}$$

$$P^*=\frac{P}{P_i},\ U=\frac{u}{u_i},\ V=\frac{v}{u_i},\ C_p=\frac{C_p}{C_{pi}},\ K^*=\frac{K}{K_i}$$

And important dimensionless parameters are:

$$\mathrm{Re}_i=\frac{\rho_i u_i H}{\mu},\ Ma_i=\frac{u_i}{\sqrt{\gamma RT_i}},\ Pe_i=\frac{u_i H}{\alpha_i},\ Kn_i=\sqrt{\frac{\pi\gamma}{2}}\frac{Ma_i}{\mathrm{Re}_i}$$

### C. Boundary Conditions

As we know, in slip flow regime that is specified with Knudsen number between 0.001 and 0.1, we have to use slip boundary conditions with Navier-Stokes equations "1-4". To do so, there are some models that recently have been validated and used by various authors such as, second order slip model [1], Langmuir [15], and some other first and second order boundary conditions. But here we will use the most general one that are Maxwell and von Smoluchowski's for slip and temperature-jump boundary conditions given by [16]. These boundary conditions are shown bellow in Cartesian form:

$$u_{fluid}-u_{wall}=\frac{2-\sigma_v}{\sigma_v}\lambda\frac{\partial u}{\partial y}+\frac{3}{4}\frac{\mu}{\rho T}\frac{\partial T}{\partial x}, \tag{10}$$

$$T_{fluid}-T_{wall}=\frac{2-\sigma_v}{\sigma_v}\frac{2\gamma}{\gamma+1}\frac{\lambda}{\mathrm{Pr}}\frac{\partial T}{\partial y} \tag{11}$$

Where we have used following definitions for Knudsen number and mean free path respectively:

$$Kn=\frac{\lambda}{L} \tag{12}$$

$$\lambda=\frac{kT}{\sqrt{2}\pi\sigma^2P} \tag{13}$$

These formulations apply to flat surfaces in non-rotating domains. As it was noted by other investigators, neglecting the influence of surface curvature or rotating motion on slip behavior leads to false prediction. Introducing necessary modifications for those cases extended, formulations have been proposed:

$$u_{fluid}-u_{wall}=\frac{2-\sigma_v}{\sigma_v}\lambda(\frac{\partial u}{\partial n}+\frac{\partial u}{\partial t})+\frac{3}{4}\frac{\mu}{\rho T}\frac{\partial T}{\partial t}, \tag{14}$$

Where $n$ and $t$ are stand for normal and tangential to surface at each point of the wall.

Choosing full accommodation ($\sigma_v=1$), there are several good agreements with experimental data in various works but they were all chosen for smooth surfaces. For nitrogen, that is our working fluid too, Table I shows values proposed by some authors.

TABLE I
FITTING PARAMETERS OBTAINED FROM SOME EXPERIMENTAL WORKS

| Previous studies | Accommodation coefficient |
|---|---|
| Porodnov(1974) [17] | 0.925± 0.014 |
| Arkilic(1997) [18] | 0.81±0.96 |
| Maurer(2003) [19] | 0.87± 0.03 |
| Colin(2004) [20] | 0.93 |
| Ewart(2007) [21] | 0.908±0.041 |

In this paper we chose $\sigma_v=0.9$ for both cases as was chosen by Ji et al [1] in their study for rectangular roughness elements and is acceptable with respect to Table I.

The other boundary conditions are at inlet and outlet of the channel illustrated bellow:

*At X=0* $\quad P^*=1, V=0, \theta=1$

*At X=1* $\quad P^*=P_{out}/P_i$

To reduce the computation work only one half of the channel is considered due to the symmetrical conditions that are applied at *Y=0.*

### D. Computational Domain and Numerical Solution Details

As we know the rarefaction and compressibility effects play important roles in gaseous flows and lead to different flow characteristics. These effects are closely related to the microchannel dimensions, inlet Mach number, and the roughness elements, etc. So we have chosen low and high inlet Mach and Knudsen numbers to highlight these effects. Our simulation is based on six models. Case 1 consists of four models while two models are included in case 2. Details of all

models are shown in Table II. All models have aspect ratio of 5 (L/H=5). The peak density, which is the number of triangular roughness elements in 0.1mm, is 10 for models of case 1 while it is 50 for models of case 2.

Air is chosen as the working gas. The inlet flow total temperature is 300 K. The wall temperature is set at 320 K.

A finite volume based CFD code was used to solve flow equations with associating boundary conditions (equations 10 and 11). Also SIMPLE algorithm has been used in body fitted coordinate system to discretize governing equations. The entire microchannel length is taken as the computational domain to investigate the effect of roughness on the flow field. Because of triangular shapes of the roughness elements we have selected triangular mesh all over the computational domain. The grids are refined near the wall region to obtain highly accurate numerical solutions around the roughness elements. For example the grids that are used for models 2, 5 have shown in Fig. 2. To evaluate the grid size effect on the accuracy of numerical solutions, grid-independence tests were performed as the grid size was refined until acceptable differences between the last two grid sizes were found. For example, we have used the following four grid sizes: 480×64, 280×48, 160×32 and 128×24. For model 1 with Kn=0.0033, Ma=0.1 and e = 0.75%, The maximal difference in fRe were 0.73%, 1.85%, 4% respectively. By balancing between the computation time and accuracy, the grid size 280×48 was selected.

TABLE II
DETAILS OF SIX MODELS USED IN THIS STUDY

| Cases | Models | Kn | Ma | Relative roughness (%) |
|---|---|---|---|---|
| Case 1 | Model 1 | 0.0033 | 0.005, 0.02 | 5, 3.75, 2.5, 1.25, smooth |
| | Model 2 | 0.0033 | 0.25, 0.4 | 5, 3.75, 2.5, 1.25, smooth |
| | Model 3 | 0.01 | 0.005 | 5, 3.75, 2.5, 1.25, smooth |
| | Model 4 | 0.033 | 0.005 | 5, 3.75, 2.5, 1.25, smooth |
| Case 2 | Model 5 | 0.0033 | 0.02 | 5, 3.75, 2.5, 1.25, smooth |
| | Model 6 | 0.0033 | 0.25 | 5, 3.75, 2.5, 1.25, smooth |

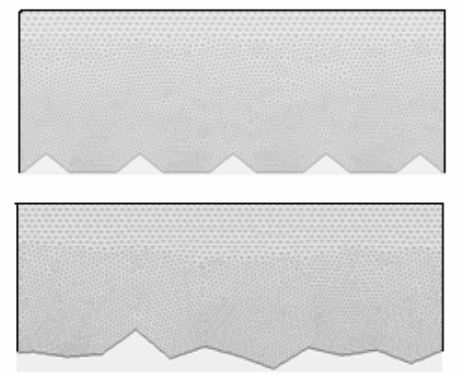

Fig. 2 The near wall grid for computational domain of model 2 (upper) and model 5 (lower)

## III. RESULTS AND DISCUSSION

In this section the effects of wall roughness on rarefied, compressible and incompressible flow are investigated for two cases that have been generated and discussed before. Although there are many parameters related with surface roughness, here we focused on *Poiseuille* number which is the most important parameter in analyzing roughness effects. Then we will compare results and discuss the differences between related models.

### A. Poiseuille Number

As we know, *Poiseuille* number is a factor for friction measurements and is defined as the product of friction factor and local Reynolds number ( $Po = f.\mathrm{Re}$ ) and we will later use equation 15 to compute it for each model.

$$f.\mathrm{Re} = \frac{-2(d\bar{P}/dx).D_h}{\mu\bar{u}} \qquad (15)$$

Where, $D_h$, is hydraulic diameter that is *2H* for the case of tow parallel plates, and $d\bar{P}/dx$ is the average pressure gradient in the flow direction. It must be noted that since pressure is decreasing through flow direction, the Knudsen number increases along a microchannel in *Poiseuille* flow. Consequently, axial velocity varies with axial distance, lateral velocity component does not vanish, streamlines are not parallel, and pressure gradient is not constant. For this case of study (two parallel plates), the acceptable value for *Poiseuille* number in conventional channels is *Po*=96 and is independent of surface roughness. But in microchannels Beskok and Karniadakis [22] recommended a simple equation fRe = 96/ (1 +6Kn) to evaluate the *Poiseuille* number for the incompressible rarefied flow, with a first order boundary condition and an accommodation coefficient of unity. The good agreement of our simulation with above relation evaluated by Beskok and Karniadakis [22] is illustrated in Fig. 3.

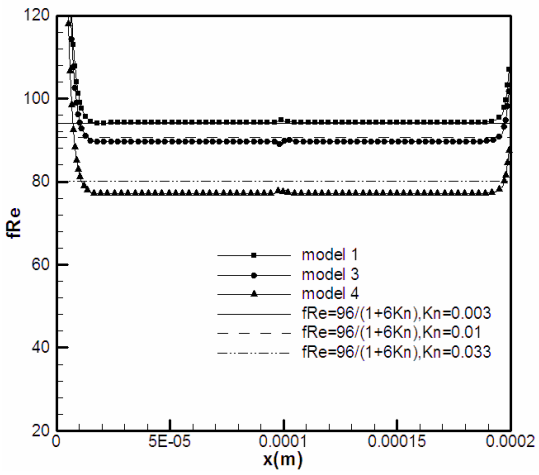


Fig. 3 Effect of Knudsen number on f.Re along smooth channels (numerical and analytical results)

Comparing results from Beskok and Karniadakis with our results indicates a similar trend except near the entrance region, where our results show an entrance effect. In general, our results are slightly lower. This comes mainly from the lower momentum and energy accommodation coefficients. The lower *Poiseuille* number is expected, since the slip condition implies less shear stress against the wall and a higher Kn means larger slip.

### *B. Slip Velocity*

Fig. 4 shows velocity distribution on centerline and the rough wall of model 5 and compares them with associated smooth models.

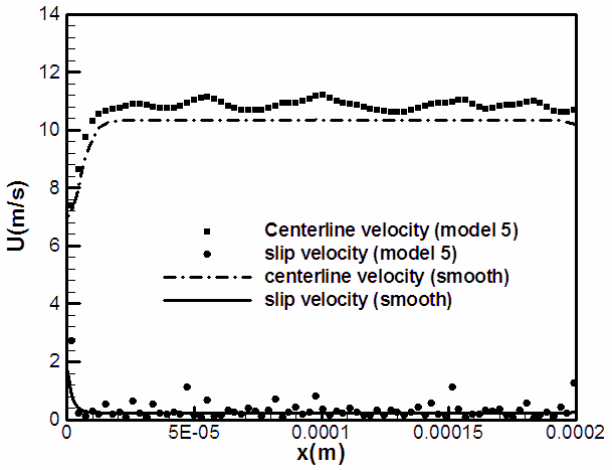


Fig. 4 Centerline and slip velocity for rough and smooth cases of model 5 (Mach=0.02, e=5%)

It can be seen that higher roughness peaks are associated with higher slip and centerline velocity compared to that of smooth channel. In addition it is found that the mass flow rate for this model will be almost 20% less than that of smooth channel because of obstruction effect. This reduction in mass flow rate is found to be 15% for model 1 that shows the sensitivity of flow field to roughness shape. The gas is compressed in the narrower space and expanded in the wider space, which results in the velocity field experiencing a periodical expansion– compression cycle.

### *C. Roughness Shape and Distribution Effects*

In this section we focus on the effect of roughness distribution on *Poiseuille* number. This is based on the comparison of pressure gradient in models of case 1 with those of case 2. Models 5 and 6 were designed to highlight these effects.

Fig. 5 and Fig. 6 show the variation of pressure gradients for models 1 and 5 with Mach number of 0.02 with different relative roughness respectively.

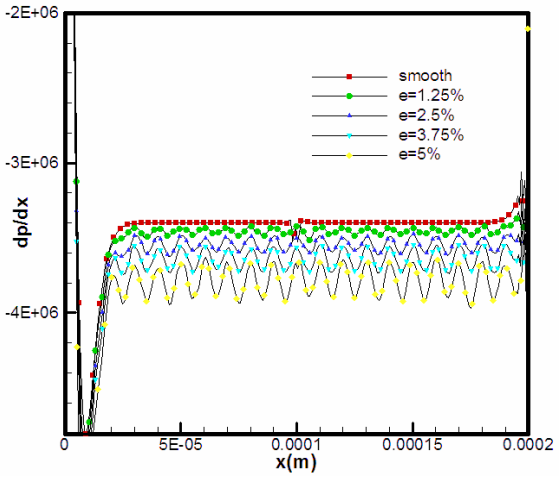


Fig. 5 Variation of pressure gradient through microchannels for models with triangular rough elements (model 1)

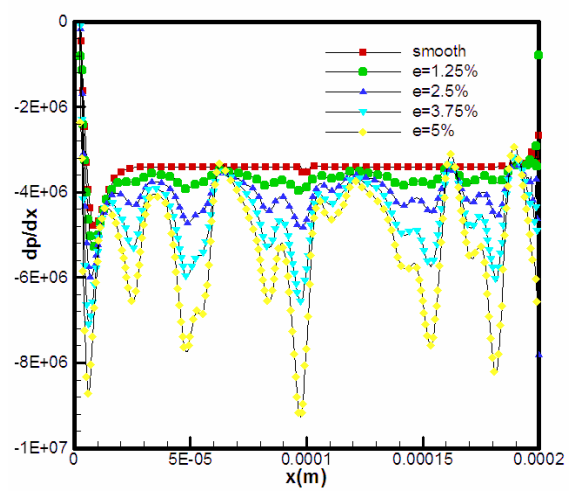


Fig. 6 Variation of pressure gradient through microchannels for models with randomly distributed rough element (model 2)

Comparison of two figures shows the high influence of roughness shape on pressure gradient. Since the conditions of two models are the same except for roughness shapes, it seems that we can not compare the results of case 1 with that of case 2 except for small relative roughness. For the case with large relative roughness the model with random roughness peaks shows extremely larger changes in pressure gradient than models with triangular roughness elements. This is because of change in flow pattern duo to perturbation caused by several large unequal obstructions exist, when relative roughness is large.

The variation of fRe against relative roughness for both incompressible and compressible flows of models 5, 6 is depicted in Fig. 7 which also compares these models with associated models of case1.

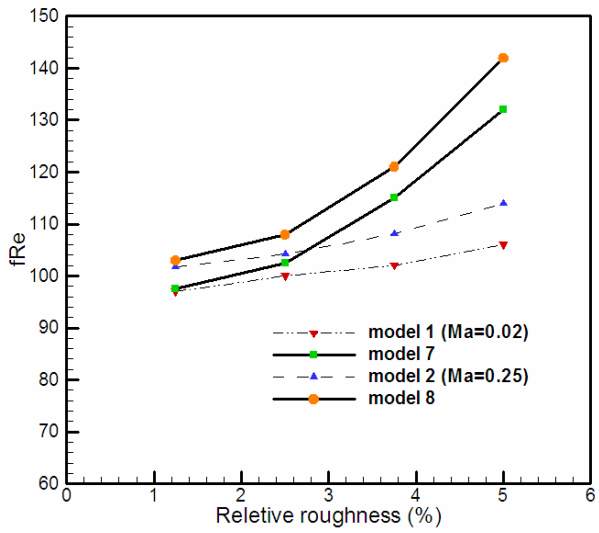


Fig. 7 Variation of average fRe against relative roughness for compressible and incompressible flow of models 7, 8 and associating models of case 1

As stated above the effect of roughness distribution on pressure gradient is significant when relative roughness is large. Since fRe is directly in relation with pressure gradient, this can be also seen in analyzing the *Poiseuille* number. In models with larger relative roughness, larger pressure gradients exist near the rough elements. Since in a model with random distribution of roughness there are peaks larger than that associated with average relative roughness, the average pressure gradient is strongly influenced by them and the *Poiseuille* number will be extremely larger. This trend can be seen in both incompressible and compressible models but since for compressible flow, pressure drop can directly affect flow field by changing density, the effect of roughness distribution is a little more for compressible flow. For example for $e$=5%, comparison of fRe for models 1, 5 shows 24% increase, since for models 2, 6 it is 26%.

## IV. Conclusion

Roughness shape and distribution effect on rarefied and compressible flow were investigated with slip flow regime taking into consideration. The following can be deduced from this study:

(1) The rough elements restrict the upstream gas flow and cause enlargement of pressure drop and *Poiseuille* number due to obstruction effect.

(2) The comparison of two studied cases show that the changing in roughness shape can leads to extremely different flow patterns except for small relative roughness.

(3) The compressible flow is more sensitive to the shape and distribution of roughness element duo to direct effects of pressure gradient on flow field.

## References

[1] Yan Ji, Kun Yuan, J.N. Chung, Numerical simulation of wall roughness on gaseous flow and heat transfer in a microchannel, Int. J. Heat Mass Transfer 49, 2006 1329–1339.

[2] S.G. Kandlikar, S. Joshi, S. Tian, Effect of channel roughness on heat transfer and fluid flow characteristics at low Reynolds numbers in small diameter tubes, in: Proceedings of NHTC_01 35th National Heat Transfer Conference, Anaheim, CA, June 2001, pp. 1–10.

[3] G.M. Mala, D. Li, Flow characteristics of water in microtubes, Int. J. Heat Mass Transfer 20 (1999) 142–148.

[4] P.Y. Wu, W.A. Little, Measurement of friction factor for the flow of gases in very fine channels used for microminiature Joule–Thomson refrigerator, Cryogenics 23 (1983) 273–277.

[5] P.Y. Wu, W.A. Little, Measurement of the heat transfer characteristics of gas flow in fine channel heat exchangers used for microminiature refrigerators, Cryogenics 24 (1984) 415–420.

[6] S. B. Choi, R. F. Barron, and R. O. Warrington, Fluid Flow and Heat Transfer in Microtubes,

[7] M. Usami, T. Fujimoto, S. Kato, Mass-flow reduction of rarefied flow roughness of a slit surface, Trans. Jpn. Soc. Mech. Eng., B 54 (1988) 1042–1050.

[8] H. Sun, M. Faghri, Effect of surface roughness on nitrogen flow in a icrochannel using the direct simulation Monte Carlo method, umer. Heat Transfer Part A 43 (2003) 1–8.

[9] G.E. Karniadakis, A. Beskok, Micro Flows, Fundamental and imulation, Springer, Berlin, 2002.

[10] E. Turner, H. Sun, M. Faghri, O.J. Gregory, Effect of surface roughness on gaseous flow through micro channels, 2000 IMECE, TD 366 (2) (2000) 291–298.

[11] W. Sugiyama, T. Sawada, K. Nakamori, Rarefied gas flow between two flat plates with two dimensional surface roughness, Vacuum 47 1996) 791–794.

[12] Sugiyama, T. Sawada, M. Yabuki, Y. Chiba, Effects of surface roughness on gas flow conductance in channels estimated by conical roughness model, Appl. Surf. Sci. 169–170 (2001) 787–791.

[13] R. Valses, J. Miana, Luis Pelegay, Luis Nunez, Thomas Putz. Numerical investigation of the influence of roughness on the laminar incompressible fluid flow through annular microchannels, Int. J. Heat Mass Transfer 50 (2007) 1865–1878.

[14] Yan Ji, Kun Yuan, J.N. Chung, Numerical simulation of wall roughness on gaseous flow and heat transfer in a microchannel, Int. J. Heat Mass Transfer 49 (2006) 1329–1339.

[15] Choi, Hyung-il, Lee, Dong-ho and Lee, Dohyung , (2005) 'Complex Microscale Flow Simulations Using Langmuir Slip Condition', Numerical Heat Transfer, Part A: Applications, 48:5, 407 - 425

[16] A. Beskok, G.E. Karniadakis, A model for flows in channels, pipes and ducts at micro and nanoscales, Microscale Thermophys. Eng. 3 (1999) 43–77.

[17] Porodnov BT, Suetin PE, Borisov SF, Akinshin VD (1974) J Fluid Mech 64:417–437

[18] Arkilic EB, Schmidt MA, Breuer KS (1997) J Microelectromech Syst 6(2):167–178

[19] Maurer J, Tabeling P, Joseph P, Willaime H (2003) Phys Fluid 15:2613–2621

[20] Colin S, Lalonde P, Caen R (2004) Heat Transfer Eng 25(3):23–30

[21] T. Ewart, P.Perrier, I.Graur, J.Gilbert, "Tangential momemtum accommodation in microtube", Microfluid nanofluid, (2007) 3:689–695

[22] A. Beskok, G.E. Karniadakis, A model for flows in channels, pipes and ducts at micro and nanoscales, Microscale Thermophys. Eng. 3 (1999) 43–77.